

Peroxodisulfate generation on boron-doped diamond microelectrodes array and detection by scanning electrochemical microscopy

D. Khamis · E. Mahé · F. Dardoize ·
D. Devilliers

Received: 4 February 2010/Accepted: 12 March 2010/Published online: 31 March 2010
© Springer Science+Business Media B.V. 2010

Abstract In this work, the electrogeneration of peroxodisulfate from a 1 M H₂SO₄ solution on boron-doped diamond microelectrodes array has been studied. The peroxodisulfate is detected at the vicinity of the boron doped diamond electrode, with the SECM probe, only when the polarization of the microarray is greater than 2.1 V versus AgCl/Ag. The main electrochemical interest of working with microarrays comes from the fact that current densities and efficiencies are comparable to those observed in the peroxodisulfate industrial production. The local Scanning Electrochemical Microscopy studies have shown that the peroxodisulfate reaction is related to a surface mediated oxidation of sulfate anions into peroxodisulfate according to a complex reactional mechanism.

Keywords Boron-doped diamond (BDD) · Peroxodisulfate electrogeneration · Scanning electrochemical microscopy (SECM) · Microelectrodes array (MEA) · Local electroanalysis · Bismuth ultramicroelectrode (UME)

1 Introduction

The electrolytical transformation of sulfate into peroxodisulfate is possible at high anodic potentials with a convenient current efficiency when the electrolyte contains a high concentration of sulfate ions (>2 M). The industrial production of peroxodisulfate is achieved by electrolysis of

sulfuric acid on Pt anodes. The two major problems are the water oxidation side-reaction decreasing the production efficiency, and the formation of a corrosion product on the Pt anodes making the purification of the electrolyte necessary. Thus, the efficiency of the process depends on the choice of the electrode material [1].

In the last few years, a particular type of conductive diamond has been a major focus in the electrochemical studies; it is the Boron-Doped Diamond (BDD). Unlike natural diamond which is monocrystalline and has a very high electrical resistivity, BDD is polycrystalline, conductive and can be used as an electrode material [2]. In fact, boron doping introduces gap states in the material, and changes its electrical conductivity towards a semimetal behaviour [3]. The electrochemical performance of the BDD film depends on the control the diamond polycrystals growth, the level of doping and the electrode pre-treatments [4–6].

The use of BDD has been expended to many electrochemical applications: reduction of nitrate in alkaline solutions [7], electrosynthesis [1, 8], anodic oxidation of cyanide [1, 3], cathodic recovery of heavy metals, enzyme based biosensing [2] and electroanalytical determinations [9–11] have been reported. However, the main application remains in the waste water treatment [3–8], basically the oxidation of inorganic and organic compounds [12].

The interest of BDD in electrochemistry comes from the fact that it has a wide potential window (~3 V in 1 M H₂SO₄ solution) [1–6] resulting from very high overpotentials to both hydrogen and oxygen evolution which makes it suitable to study a larger variety of analytes in aqueous electrolytes, i.e. those that usually react beyond the decomposition of water, such as the peroxodisulfate. Furthermore, on the BDD, the background current is very low and a high stability in severe oxidizing conditions is observed [1, 6]. In contrast to metallic electrodes, it is

D. Khamis · E. Mahé (✉) · F. Dardoize · D. Devilliers
Laboratoire de Physicochimie des Électrolytes, Colloïdes et Sciences Analytiques (PECSA, UMR 7195), Université Pierre et Marie Curie, 4 Place Jussieu, 75005 Paris, France
e-mail: eric.mahe@upmc.fr

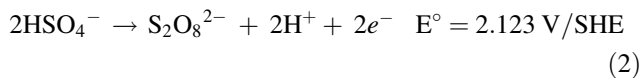
generally assumed that no passivating layers are formed on BDD surfaces in the electroactive domain [2], although a submonolayer of oxygenated surface groups may be present at higher potentials [13]. Thus, BDD electrodes require less surface cleaning and they are suitable for microelectrode arrays, for which polishing and conditioning the surface can be difficult.

The mechanism of the formation of peroxodisulfate from sulfate anions on platinum electrodes has been widely studied [14], as well as their reduction on different electrode material [15–17]. Two mechanisms have been proposed for the generation of peroxodisulfate.

The first model, proposed by Smit and Hoogland [14], considers a direct oxidation process at the electrode:

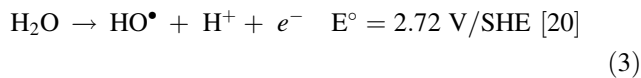


Due to the influence of the pH on the kinetics observations, the protonation of sulfate has been taken into account by Stark [18]. The mechanism should imply both species SO_4^{2-} and HSO_4^- . The following equation must be taken into account:

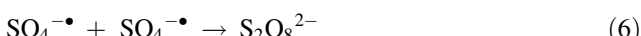


Furthermore, Smit and Hoogland [19] have pointed out a competitive phenomenon between the oxide formation and the adsorption of SO_4^{2-} on platinum electrodes. The sulfate adsorption followed by its oxidation is responsible of the decrease of the oxygen evolution reaction (OER) rate due to a decrease of the electrode active surface. Smit et al. [14] have shown that the surface of the platinum electrode is progressively replaced by patches of adsorbed SO_4^{2-} on which $\text{S}_2\text{O}_8^{2-}$ formation proceeds instead of the oxygen evolution.

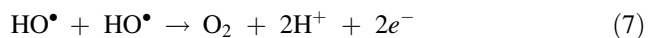
The second model involves an indirect oxidation process in aqueous solutions. It has been shown that HO^\bullet is readily formed at BDD anodes [3]. The first step on BDD is water oxidation leading to very reactive hydroxyl radicals:



The electrogenerated hydroxyl radical can react with the electrolyte [3]. According to Caro [20], Palme [21] and Kolthoff [22], HSO_4^- and H_2SO_4 are the main species involved in the following steps:



According to this model, a side reaction is also possible due to the coupling of hydroxyl radicals:



After the first description of peroxodisulfate production on BDD electrodes [1], the mechanism has been discussed by Serrano et al. [6]. More recently, Provent et al. [23] have used BDD microelectrode array (MEA) in order to obtain mechanistic informations from voltammetric measurements for the sulfate oxidation process. In fact, as shown by the described models, there is always a concurrent oxidative process involved in the peroxodisulfate anodic production on BDD electrodes. Two methods could be proposed in order to extract mechanistic informations after deconvolution of the simultaneous processes involved:

- (i) The first, used by Provent et al. [23] based on reverse electrochemical methods on BDD MEAs, like cyclic voltammetry (CV) or double-potential step chronoamperometry (DPS-CA). According to this method, the detection of the produced peroxodisulfate is done on the BDD electrode on which it has been previously produced.
- (ii) The other possibility is to use a generator-collector electrodes assembly. According to this electrochemical method, all the oxidized species produced at the BDD anode are detected by electrochemical reduction at the probe electrode of a Scanning Electrochemical Microscope (SECM). The Substrate Generation/Tip Collection (SG-TC) technique consists in a steady state generation of a species at the microelectrode substrate when the ultra microelectrode (UME) probe of the SECM can detect the product previously obtained at the substrate.

Indeed SECM is a very powerful electrochemical technique, widely used for studying redox reactions at solid–liquid interface. It allows analytical imaging and kinetic studies. Thanks to the efficiency of the method, nano and microstructured surfaces like metallic nanoparticles and carbon nanotubes have been characterized [24, 25]. Local electroanalytical studies in confined microsystems (i.e. SG-TC mode) are useful because high collection efficiency can be reached. Thus it allows a lower detection limit.

Therefore, in this work, we propose to get results from a generator-collector electrochemical method in order to elucidate the mechanism of production of peroxodisulfate at BBD microdisks arrays anodes. A SECM, with microelectrode probe, has been used in order to obtain an adaptative generator-collector cell when combined with a single BDD microelectrode chosen among the MEA. This strategy gives the advantage to control independently the generator electrode to collector electrode distance and to operate the reduction step (analytical detection on the SECM probe) on a different material from the generator electrode (BDD microelectrode). The obtained results

could be compared toward those obtained with the reverse electrochemical methods (CV, DPS-CA).

2 Experimental

2.1 Chemicals

Ferrocenecarboxylic acid > 97% (Aldrich, MO, USA), H₂SO₄ 96% and HClO₄ 64% (Carlo Erba, Spain), K₂S₂O₈ 99% (ProLabo, France) and Bi(NO₃)₃ pentahydrate 98.5% (Merck, Germany) were used as received. Deionized water was obtained with a deionizing system (Maxima, Elga Co.).

2.2 Apparatus

All electrochemical experiments were performed at room temperature, in a conventional three-electrode arrangement using a CHI 910B SECM (CH Instruments Inc., Austin, Texas, USA), which incorporates a bipotentiostat. A 1 mm diameter Pt wire and a Ag/AgCl/KCl(saturated) electrode served as the counter and the reference electrodes, respectively. A Nanoscope IIIA (Veeco Instruments Inc., USA) atomic force microscope (AFM) was used for the determination of the geometric characteristics of the BDD MEA (Tapping mode; tip resonance: 325 kHz; scan rate: 0.5 Hz).

2.3 Electrodes

2.3.1 Probe electrodes

Gold or platinum microdisk electrodes (diameter: $2a = 10 \mu\text{m}$) (CH Instruments, Austin, Texas, USA) embedded in a thin glass fitting were used as the SECM tips. We have also prepared a Pt UME modified by Bi film using a 10 μm Pt disk as the base electrode. The Bi microfilm was electrochemically deposited from a 0.01 M Bi(NO₃)₃ in 0.1 M HClO₄ solution using a potential step technique with the following parameters: 5 s at 0.4 V + 20 s at -0.15 V (20 cycles) to efficiently initiate the deposition. Then, 20 scans at 50 mV s⁻¹ were performed between -0.05 and -0.120 V, in order to homogenize and improve the surface of the just-made Bi microfilm [26–28].

2.3.2 Preparation and description of the microelectrodes arrays

The BDD MEAs used in this work were provided by the CSEM (Centre Suisse d'Electronique et de Microtechnique SA), Neuchâtel, Switzerland and Adamant Technologies

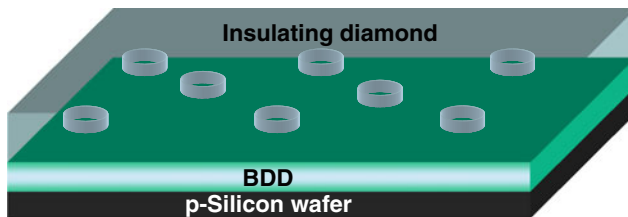


Fig. 1 Representative scheme of the microelectrodes network. The distance between the centres of two neighbouring BDD disks is 150 μm and the diameter of the disks is 5 μm

SA, Neuchâtel, Switzerland. The detailed method for the preparation of the samples using the HF-CVD technique is described in previous works [29–32]. Briefly, it consists in a thermal activation of a gas phase by a highly heated filament. In a continuously pumped vacuum chamber reactor, the precursor gases (0.5–2.5% methane in hydrogen) are dissociated by thermal energy from the hot tungsten filament (2,200–2,600 °C), resulting in the formation and the diffusion of the reactive species toward the substrate surface. Then, a carbon film is formed by grains nucleation and coalescence. To obtain BDD, trimethylboron is added to the precursor gases with a concentration depending on the doping level needed. Typical boron concentration ranges from 500 to 8,000 ppm. The sample used in the present study is a p-silicon substrate on which a BDD and an insulating diamond layers were deposited successively. Then, by laser ablation, holes were made in the upper layer revealing BDD disks (diameter $2b = 5 \mu\text{m}$) on the surface. The holes are 150 μm distant from each other creating a centered hexagonal configuration. A sketch representation of the sample is given in Fig. 1.

2.4 Electrochemical experiments

2.4.1 Scanning electrochemical microscopy

The main operation mode in SECM is the feedback mode. When the UME is far from the substrate surface and polarized at a potential that permits the redox reaction, the tip steady state current is given by

$$i_{\text{tip},\infty} = 4nFDCa \quad (8)$$

where n is the number of electron transferred, F the Faraday constant, a the tip radius, D the diffusion coefficient of the electroactive species and C its concentration. When the substrate is insulating, the tip current decreases when the UME is approached closer to the substrate. This is linked to a “negative feedback”. On the contrary, when the substrate is conductive and polarized at a potential that permits the reverse redox process, the tip current increases and a “positive feedback” takes place as shown in Fig. 2a. When the electroactive species is electrochemically

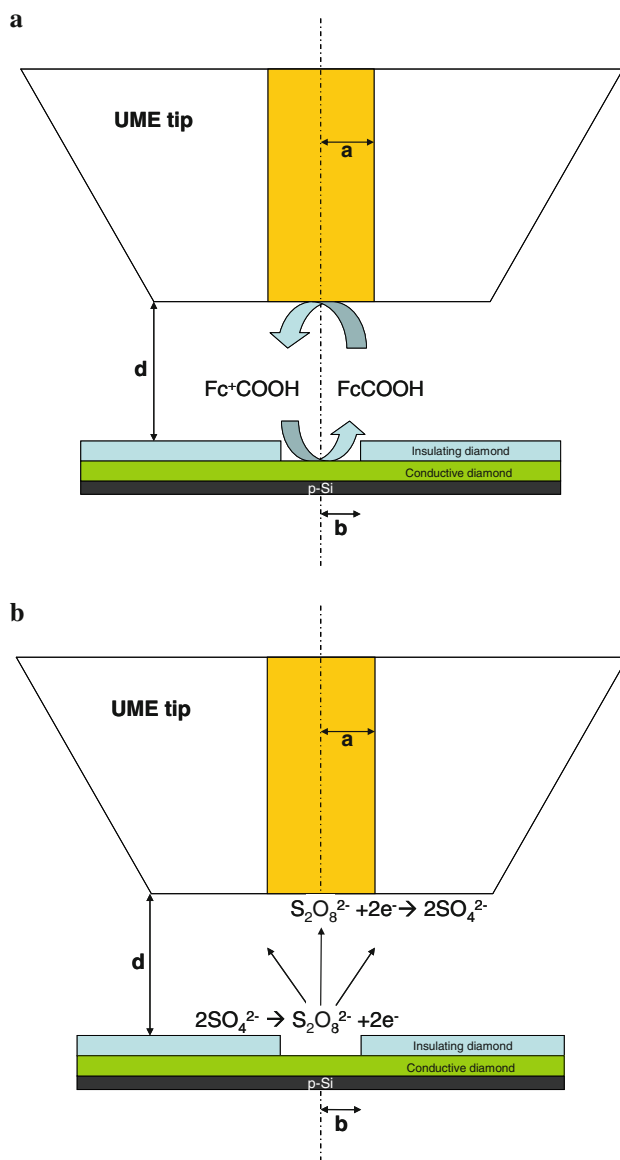


Fig. 2 **a** Feedback operation mode of SECM used for BDD MEA screening with the FcCOOH solution. **b** Substrate generation/tip collection (SG/TC) mode of the SECM used for detection and local electroanalysis of peroxodisulfate electrogeneration on the BDD MEA

generated on the substrate, and detected on the UME tip, it is the Substrate Generation/Tip Collection (SG/TC) mode. More details on SECM principles are given in the literature [33–35].

Figure 2b shows the operational scheme of the SG-TC mode of SECM experiments [36] employed for the study of the oxidation of concentrated sulfuric acid into peroxodisulfate on BDD microelectrodes. The produced peroxodisulfate is reduced on the UME leading to a current detected only above the BDD microdisks. Before imaging, the tilt of the substrate was adjusted until an acceptable flatness was

reached; i.e. the vertical to horizontal displacement is estimated by the variation of the tip current as $\Delta i_{\text{tip}}/\Delta x$ (or Δy) $\leq 1 \text{ nA mm}^{-1}$. The tip was brought at about $d = 40\text{--}50 \mu\text{m}$ from the substrate with the ferrocenecarboxylic (FcCOOH) solution and at about $10\text{--}20 \mu\text{m}$ with the H_2SO_4 solution. The SECM images provide a simple evaluation of the array since the microdisks appear as spots with higher currents due to the positive feedback. Thus, the images may be used to precisely evaluate the position of one of the microdisks. The tip is then carefully moved and positioned at the coordinates corresponding to the centre of the chosen microdisk, in order to perform the local experiments on that single disk.

2.4.2 Square wave voltammetry

All the square wave technique experiments were done with the following parameters:

A rest time of 5 s preceded each run. A potential increment of 0.004 V was used. The potential signal had an amplitude of 0.05 V and a frequency of either 25 or 100 Hz.

3 Results and discussion

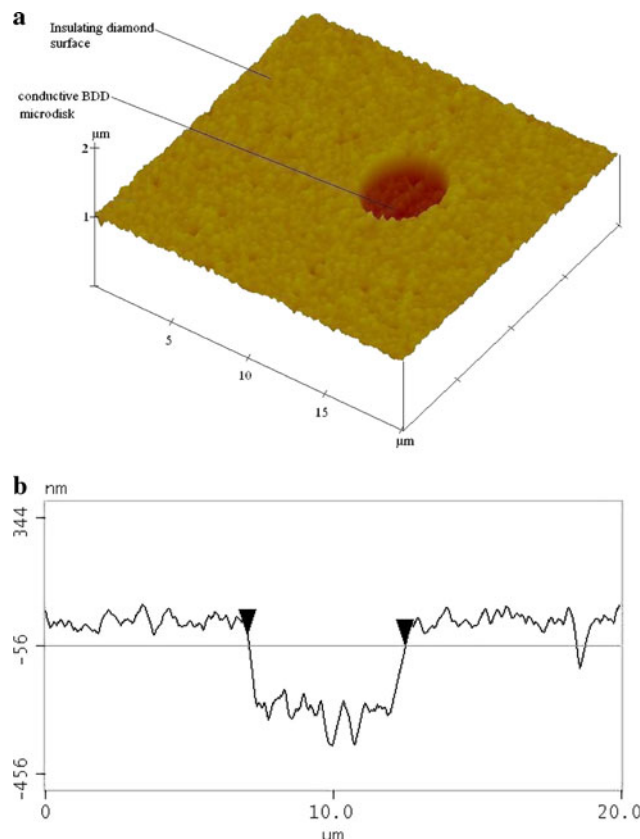
3.1 Characterization of the BDD microelectrodes array

3.1.1 Atomic force microscopy

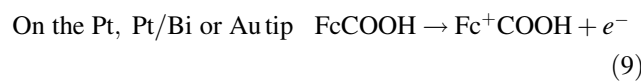
An AFM study was necessary to know the exact dimension of the network holes, i.e. the diameter of the microdisk BDD electrodes. An AFM image of the sample, obtained in tapping mode is given in Fig. 3a as well as a section analysis in Fig. 3b. The BDD microelectrode appears as a microdisk embedded in the insulating diamond top surface. Each electrode has a $5 \mu\text{m}$ diameter. The average depth of the hole is about 300 nm. The ratio diameter/depth is larger than 15; thus the microdisk electrodes can be considered as non-recessed.

3.1.2 SECM in $\text{FcCOOH}/\text{phosphate buffer}/\text{KCl}$

A SECM scanning of the array was made in feedback mode, in 1 mM ferrocenecarboxylic acid (FcCOOH)/0.01 M phosphate buffer/1 M KCl solution, using consecutively a Pt, Pt/Bi microfilm and an Au UME with $10 \mu\text{m}$ as diameter. The tip was polarized at 0.55 V versus Ag/AgCl and the substrate was kept at its open circuit potential (OCP) of 0.235 V versus Ag/AgCl . The images obtained (Fig. 4) show dark spots on a light surface, related to higher currents (positive feedback) on the BDD



microelectrodes. Our voltammetric measurements give a value of $E_{\text{Fc}^+ + \text{COOH}/\text{FcCOOH}}^0$ equal to 0.35 V versus Ag/AgCl which is coherent with the literature [37]; the redox reactions are:



As shown in Fig. 4, the three types of UME material are usable for SECM imaging. However, it must be precised that with the Pt, the early hydrogen formation occurs and is not suitable for scanning a large reduction window. To our knowledge, it is the first time that a bismuth UME was used as a tip for SECM investigations. However, with the Pt/Bi_{microfilm} UME, the reproducibility of peroxodisulfate detection was not very good. This was due to the poor properties of the bismuth film: the conditions of the electrodeposition were not optimized and lead to a heterogeneous film with an incomplete covering of the tip. Furthermore, the peroxodisulfate detection may only occur at potentials where the Bi film can be electrochemically dissolved. On the contrary, the Au tips allowed us to work at low reduction potentials. Since we were interested in

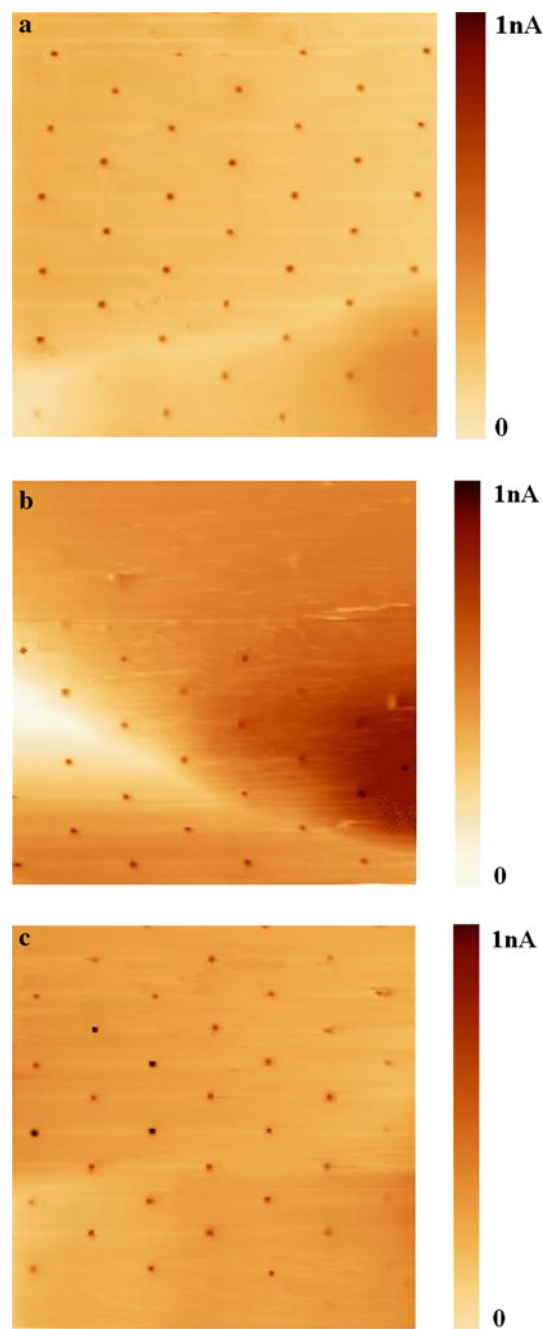


Fig. 4 SECM images ($900 \times 900 \mu\text{m}$) of the BDD microelectrodes array, with a $10 \mu\text{m}$ diameter Pt (a), Pt/Bi_{microfilm} (b) or Au (c) UME as the collection tip polarized at 0.55 V, in a 1 mM FcCOOH/0.01 M phosphate buffer/1 M KCl solution. The substrate was at its OCP (0.235 V vs. Ag/AgCl)

detecting the reduction of peroxodisulfate, Au tips have been chosen for all the following experiments.

3.1.3 SECM in H_2SO_4

A steady state linear sweep voltammetry was performed in a 1 M H_2SO_4 solution, in order to verify the electroactive

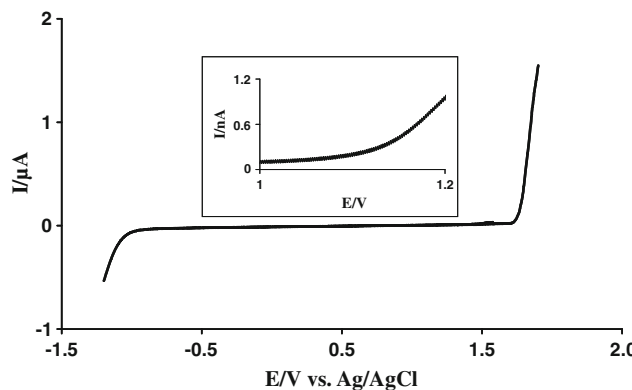
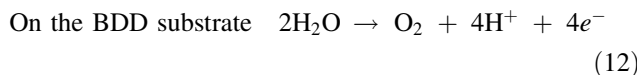
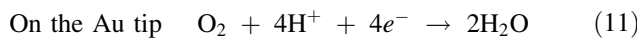


Fig. 5 Steady state linear sweep voltammetry on the BDD microelectrodes array in a 1 M H_2SO_4 solution. Inset: enlargement of the curve in the 1.0–1.2 V region

domain of the BDD microelectrodes on the array. The corresponding voltammogram is presented in Fig. 5.

Our aim was to study the local electroactivity of the microarray in the H_2SO_4 solution. So, we needed to be able to position the tip with respect to the substrate and image directly within the H_2SO_4 solution, in order to avoid affecting the positioning precision that can arise from changing the solution once the tip is positioned. As a redox mediator was not present in the solution to create the SECM feedback loop, we chose to base our imaging on the oxygen electrochemical reactions. On the Au tip, the oxygen reduction (11) occurs starting -0.1 V versus Ag/AgCl , when the water oxidation (12) takes place at the BDD microdisks polarized at a potential larger than 1.1 V as seen in the inset of the Fig. 5. The resulting SECM image is presented in Fig. 6a. Figure 6b presents the current profile above one of the BDD microelectrodes along the x axis. The apparent diameter of the BDD microelectrode (width of the current peak at half-maximum), is dependent on the approach distance from the surface. In this case, with a $10 \mu\text{m}$ diameter tip positioned at about $10 \mu\text{m}$ from the substrate surface, a doubling of the real diameter is observed on the recorded image.



3.2 Electroanalytical detection of peroxodisulfate species on Au UME

In order to be able to identify the presence of the peroxodisulfate species electrogenerated on the BDD surface, according to the principle described previously in Fig. 2, a preliminary study of the reduction of $\text{K}_2\text{S}_2\text{O}_8$ (KPS) in potassium perchlorate on the Au UME was necessary.

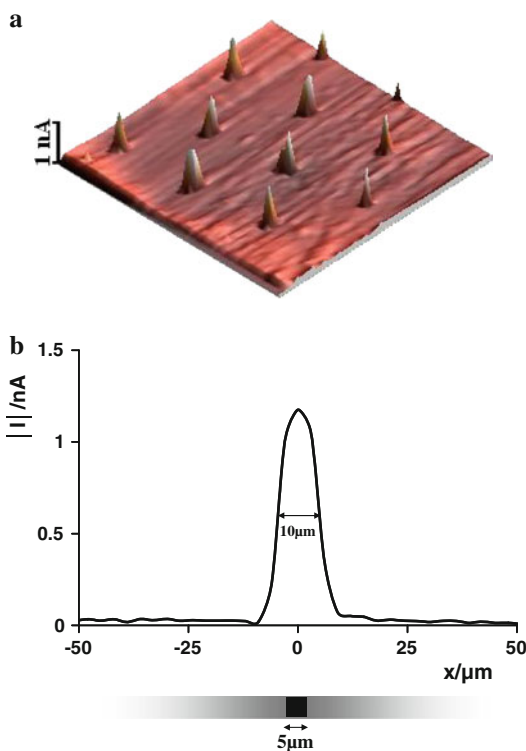


Fig. 6 **a** SECM image ($500 \times 500 \mu\text{m}$) of the BDD microelectrodes array, with a Au UME ($10 \mu\text{m}$ diameter) as the collection tip polarized at -0.3 V, in a 1 M H_2SO_4 solution. The BBD microdisk ($5 \mu\text{m}$ diameter) substrate is polarized at 1.1 V versus Ag/AgCl . **b** Current profile on the x axis above one of the microdisks

Figure 7 shows a square wave electroanalysis of KPS solutions at different concentrations of 0.01 , 0.015 and 0.02 M in 0.1 M potassium perchlorate. The intensity of the peak at about -0.2 V, increases linearly with the concentration of $\text{S}_2\text{O}_8^{2-}$. Thus, that peak is attributed to the peroxodisulfate reduction.

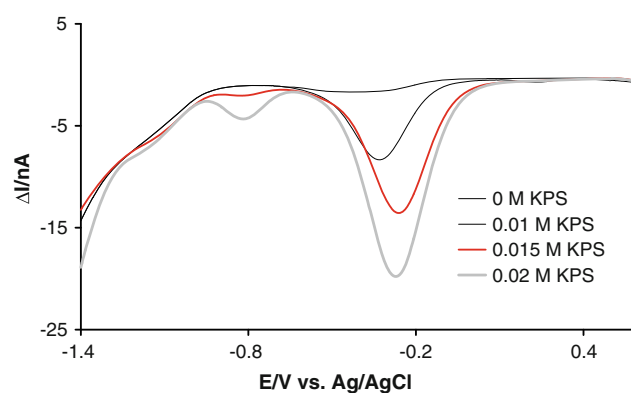


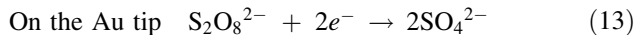
Fig. 7 Square wave voltammetry, with 25 Hz as the signal frequency, at a $10 \mu\text{m}$ diameter Au UME. Potassium peroxodisulfate (KPS) solutions in 0.1 M potassium perchlorate

3.3 Local electroanalytical study of peroxodisulfate formation on BDD microelectrode

After the SECM imaging step, images were used to position the tip in front of the centre of one BDD microdisk on the array and at 10–20 μm from the substrate surface as described in paragraph 2.3.1. All the following results were obtained with those positioning conditions. We studied the possibility of working locally in a confined microsystem.

3.3.1 Cyclic voltammetry

A cyclic voltammogram (CV), obtained with a SECM Au tip when the BDD substrate is held at 0.5 or 2.2 V versus Ag/AgCl with a scan rate of 50 mV s⁻¹, is presented in Fig. 8. When the substrate potential is 0.5 V the voltammogram presents only one large reduction peak at approximately -0.8 V. When we apply 2.2 V to the substrate an extra peak appears at -0.2 V. According to the literature [15–17, 38] and to our previous results presented in paragraph 3.2, we can conclude that peroxodisulfate is detected at -0.2 V according to reaction (13) when the BDD is polarized at 2.2 V. This means that S₂O₈²⁻ has been previously formed on the BDD microdisks of the array according to reaction (1).



The current measured in CV has a faradaic and capacitive contribution. The latter cannot be extracted by a simple method. Thus, we opted for square wave voltammetry (SWV) in which a differential current is measured for avoiding the capacitive problem. Thus we could extract

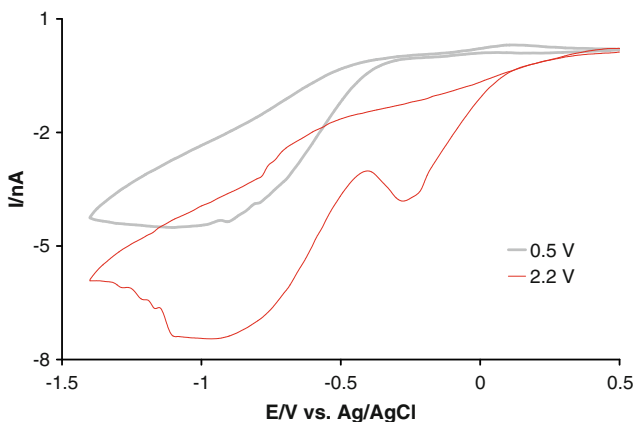


Fig. 8 Cyclic voltammetry on the 10 μm diameter Au SECM tip, when the BDD substrate was held at 0.5 or 2.2 V versus Ag/AgCl, in a 1 M H₂SO₄ solution. Scan rate $v = 50 \text{ mV s}^{-1}$. The tip was positioned above the centre of one BDD microdisk chosen on the array, at about 10 μm from its surface

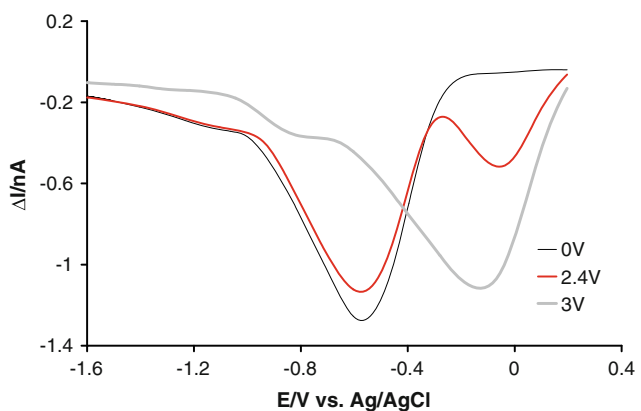


Fig. 9 Square wave voltammetry, with 25 Hz as the signal frequency, at a 10 μm diameter Au SECM tip. The BDD substrate was held at 0, 2.4, or 3 V versus Ag/AgCl, in a 1 M H₂SO₄ solution. The tip was positioned above the centre of one BDD microdisk chosen on the array, at about 10 μm from its surface

kinetic parameters giving more information about the reaction mechanism.

3.3.2 Square wave voltammetry

The position of the peaks and their attribution are similar to that deduced from the CV experiments, but the mechanistic phenomena here are more interpretable since the evolution of the peaks is clearer, because it is not disturbed by the capacitive current. The square wave voltammograms presented in Fig. 9 were realized with the same SECM positioning conditions. Three potentials (0, 2.4, and 3 V vs. Ag/AgCl) were applied successively at the BDD electrode in the 1 M H₂SO₄ solution. The peroxodisulfate reduction peak at -0.2 V appears frankly on the 2.4 V curve, and increases with the applied potential. This is in agreement with the literature where the electrolytical formation of peroxodisulfate from sulfate anions is reported to be possible at very high potentials with a lowest threshold of 2 V and increases as the anodic potential increases [1, 2].

The peak at -0.6 V is not due to the persulfate system and will be discussed in the next section.

The same interpretation can be given to the experiments reported in Fig. 10, in which higher frequency signal (100 Hz) has been chosen, allowing us to detect intermediary species with shorter lifetime. The enlargement of the peaks in these kinetic conditions proves the existence of a complex multi-step mechanism involving surface intermediates.

4 Discussion

Considering our results, it is possible to draw out a new description of the various processes occurring during the

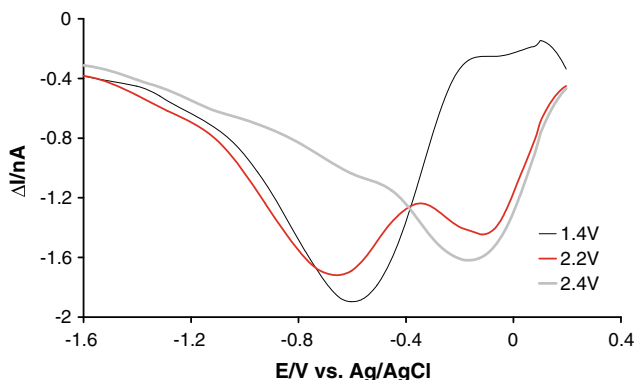
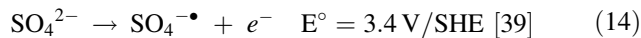


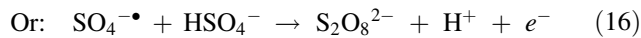
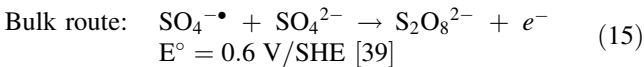
Fig. 10 Square wave voltammetry, with 100 Hz as the signal frequency, at a 10 μm diameter Au SECM tip. The BDD substrate was held at 0, 2.4, or 3 V versus Ag/AgCl, in a 1 M H_2SO_4 solution. The tip was positioned above the centre of one BDD microdisk chosen on the array, at about 10 μm from its surface

production of peroxodisulfate from concentrated sulfuric acid aqueous solutions.

It should be possible to identify the oxidizing species electrochemically produced at the BDD microelectrode. The first possible candidate is the direct sulfate radical production given by:

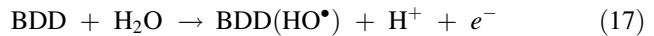


The following steps are also reported:



However, the production of the highly oxidant sulfate radical is not obtained for the polarization conditions experienced in this study.

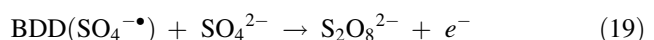
The other hypothesis that we can take into account is the electrochemical production of a surface activated state corresponding to a redox couple at the diamond electrode surface. As it has been shown by Kapalka et al. [13], the electrochemical reactivity of the oxygen species at the boron doped diamond electrodes is characterized by a pre-OER potential domain for which surface oxidation of the BDD electrode can occur. This pre-OER potential domain appears in acid media (HClO_4 1 M) for a polarization from 1.8 to 2.4 V versus AgCl/Ag. For potentials larger than 2.4 V versus AgCl/Ag, OER is clearly the main phenomenon. This pre-OER irreversible behaviour has been attributed to a semi-hydroquinone/semi-benzoquinone functional group on BDD electrodes [13]. This surface reaction has been formally written as:



According to our measurements in SG-TC SECM mode, it has been clearly shown that the reduction of the peroxodisulfate at the gold tip occurs only when the BDD is polarized at potentials larger than 2.1 V versus AgCl/Ag. It can be proposed that the persulfate production route is possible through an oxygen activated surface formed under the pre-OER polarization conditions.

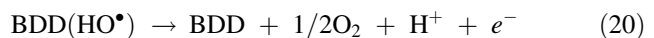
We can use the simplified mechanism of the sulfate oxidation on BDD electrodes taking into account the surface activated state adapted from [13]. The first electrochemical step consists in the formation of the activation site when the potential is about 2.1 V versus AgCl/Ag in the pre-OER region according to Eq. 17 [13].

The following mediated surface chemical steps are responsible for the formation of peroxodisulfate:



The surface site $\text{BDD}(\text{SO}_4^{\cdot-})$ is not as oxidative as $\text{SO}_4^{\cdot-}$, but is sufficient to take part in the $\text{S}_2\text{O}_8^{2-}$ formation.

Finally, the electrochemical deactivation of the hydroxylated sites consisting in an oxidation of the diamond electrode when the potential is about 2.4 V versus AgCl/Ag occurs and leads to the OER:



The overall peroxodisulfate formation process corresponds to the reaction (1) [14, 39].

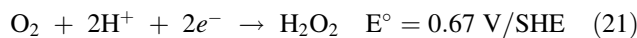
The whole process is highly dependent on the mediated electrode surface generation of intermediate $\text{BDD}(\text{SO}_4^{\cdot-})$ which seems possible at a potential for which the direct electrochemical formation of $\text{SO}_4^{\cdot-}$ appears to be impossible. The dependence of the nature of the anode toward the $\text{S}_2\text{O}_8^{2-}/\text{SO}_4^{2-}$ system has already been extensively studied on other electrode materials, especially bismuth [15, 17]. The main explanation involved is the great facility of sulfate adsorption.

As a first hypothesis, the second reduction peak obtained on the gold tip at -0.6 V versus AgCl/Ag can be related to the oxygen reduction reaction because it has been also observed in perchloric acid. The overall four electrons reaction is not known to occur mechanistically:

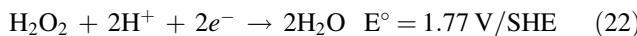


It is well known that the oxygen reduction on gold electrodes generally occurs according to a two-step mechanism [34, 40, 41].

The first step of the two-electron oxygen reduction reaction on gold electrode is:



The second step is the H_2O_2 reduction to produce H_2O :



An additional side reaction can occur: H_2O_2 disproportionation, depending on the electrolyte composition and/or the presence of a catalyst:



In fact, on the gold SECM probe the oxygen reduction is observed in H_2SO_4 1 M at -0.1 V versus AgCl/Ag . This reaction is not observed because in the SG-TC method the volume of solution in which the reactions occur is confined to a very small space. After several reduction cycles, the confined volume of solution is depleted in dissolved oxygen. Thus, the reduction of oxygen is not anymore observed at the gold UME. In those conditions, the ORR does not interfere with the detection of peroxodisulfate at the gold tip as seen in Fig. 9.

Therefore, the second peak obtained on the gold tip at -0.6 V versus AgCl/Ag can't be attributed to reduction of dissolved oxygen. In fact, for this potential the reduction of the electrolyte (H_2SO_4) begins to occur according to the following equation:



This irreversible system gives rise to a peak (on the differential current voltammogram) due to the SWV waveform as it was shown by Daniel et al. [42] and confirmed by the analysis of the individual forward and reverse SWV currents by Fatouros and Krulic [43].

5 Conclusions

The aim of this paper was to investigate the mechanism of production of peroxodisulfate with the help of new tools like SECM, which bring new powerful data and a local probing of electrocatalysis aspects.

We have proved that conventional SECM feedback mode could be used for imaging a BDD MEA. We have shown that bismuth microelectrodes can be prepared and used as new SECM probes for imaging with a reduction on the tip, as well as gold UME.

A Substrate Generation/Tip Collection configuration has been used to characterize the peroxodisulfate formation at BDD MEA. Those SECM investigations give new important informative data on the mechanism of sulfate oxidation. We have identified a reactional process in the pre-OER polarization domain on BDD MEA that is related to a surface mediated oxidation of sulfate anions into peroxodisulfate. The peroxodisulfate is detected at the vicinity of the BDD

electrode, with the SECM probe, only when the polarization of the BDD MEA is larger than 2.1 V versus AgCl/Ag . The main electrochemical interest of working with microarrays comes from the fact that current densities and efficiencies are comparable to those observed in the peroxodisulfate industrial production.

This paper has been a contribution to the in-expansion domain of electroanalytical studies on BDD microelectrodes [44].

References

- Michaud P-A, Mahé E, Haenni W, Perret A, Comminellis Ch (2000) *Electrochim Solid-State Lett* 3:77
- Luong J, Male K, Glennon J (2009) *Analyst* 134:1965
- Michaud P-A, Panizza M, Ouattara L, Diaco T, Foti G, Comminellis Ch (2003) *J Appl Electrochem* 33:151
- Salazar-Banda G, Andrade L, Nascente P, Pizani P, Rocha-Filho R, Avaca L (2006) *Electrochim Acta* 51:4612
- Mahé E, Devilliers D, Ch Comminellis (2005) *Electrochim Acta* 50:2263
- Serrano K, Michaud P-A, Comminellis Ch, Savall A (2002) *Electrochim Acta* 48:431
- Bouamrane F, Tadjeddine A, Butler JE, Tenne R, Lévy-Clément C (1996) *J Electroanal Chem* 405:95
- Iniesta J, Michaud P-A, Panizza M, Comminellis Ch (2001) *Electrochim Commun* 3:346
- Haenni W, Baumann H, Ch Comminellis, Gandini D, Niedermann P, Perret A, Skinner N (1998) *Diam Relat Mater* 7:569
- Fujishima A, Rao N, Popa E, Sarada B, Yagi I, Tryk D (1999) *J Electroanal Chem* 473:179
- Medeiros R, de Carvalho A, Rocha-Filho R, Fatibello-Filho O (2008) *Talanta* 76:685
- Vatistas N, Comminellis Ch (2010) In: Comminellis Ch, Chen G (eds) *Electrochemistry for the environment*, Chap 9. Springer Verlag, New York
- Kapalka A, Foti G, Ch Comminellis (2007) *Electrochim Acta* 53:1954
- Smit W, Hoogland JG (1971) *Electrochim Acta* 16:1
- Jäger R, Kallip S, Grososki V, Lust K, Lust E (2008) *J Electroanal Chem* 622:79
- Climent V, Macia MD, Herrero E, Feliu M, Petri O (2008) *J Electroanal Chem* 612:269
- Samec Z, Bittner A, Doblhofer K (1997) *J Electroanal Chem* 432:205
- Stark W (1989) *Z Phys Chem* 29:385
- Smit W, Hoogland JG (1971) *Electrochim Acta* 16:961
- Caro H (1898) *Z Angew Chem* 11:845
- Palme H (1920) *Z Anorg Chem* 112:97
- Kolthoff I, Miller I (1951) *J Am Chem Soc* 73:3055
- Provent C, Haenni W, Santoli E, Rychen P (2004) *Electrochim Acta* 49:3737
- Zoski C, Luman C, Fernandez C, Bard A (2007) *Anal Chem* 79:4957
- Xiong H, Guo J, Amemiya Sh (2007) *Anal Chem* 79:2735
- Valsiunas I, Gudavičiute L, Steponavicius A (2005) *Chemja* 16:21
- Valsiunas I, Gudavičiute L, Kapocius V, Steponavicius A (2006) *Chemja* 17:11
- Valsiunas I, Mieciškėnas P, Gudavičiute L, Steponavicius A (2006) *Chemja* 17:35

29. Provent Ch, Santoli E, Rychen Ph. <http://www.adamantec.com/datas/SR03-64.pdf>
30. Madore Ch, Rohner C, Duret A, Sollberger F, Santoli E, Skinner N, Tang XM, Haenni W. <http://www.adamantec.com/datas/SR99-65.pdf>
31. Duo I (2003) Thesis no 2732: EPFL-1015, Lausanne, Switzerland
32. Marselli B (2004) Thesis no 3057: EPFL-1015, Lausanne, Switzerland
33. Sanchez-Sanchez C, Rodriguez-Lopez J, Bard A (2008) Anal Chem 80:3254
34. Sanchez-Sanchez C, Bard A (2009) Anal Chem 81:8094
35. Bard A, Mirkin M (2001) Scanning electrochemical microscopy. Marcel Decker, New York
36. Minguzzi A, Alpuche-Alves M, Rodriguez Lopez J, Rondinini S, Bard A (2008) Anal Chem 80:4055
37. Ryabov A, Goral V, Gorton L, Csoregi E (1999) Chem Eur J 5:961
38. Sawyer D (1991) Oxygen chemistry. Oxford University Press, New York, p 24
39. Memming R (1969) J Electrochim Soc 116:785
40. Yeager E (1984) Electrochim Acta 29:1527
41. Genshaw M, Damjanovic A, Bockris J (1967) J Electroanal Chem 15:163
42. Daniele S, Bragato C, Baldo A (2002) Electrochim Commun 4:374
43. Fatouros N, Krulic D (2002) J Electroanal Chem 520:1
44. Fujishima A, Einaga Y, Narasinga Rao T, Tryk D (2005) Diamond electrochemistry. Elsevier, Amsterdam